



A Potential Parameter for A Non-Darcy Form of Two-Phase Flow Behaviour, Compressibility Related

Bashir Busahmin^{1*} and Brij Maini²

¹ Petroleum and Chemical Engineering, Universiti Teknologi Brunei, Brunei Darussalam.

² Chemical and Petroleum engineering, University of Calgary, Canada.

*Corresponding author: bashir.abusahmin@utb.edu.bn

Abstract

Numerous scientists did their studies and conducted various laboratory experiments related to a non-Darcy behavior of a two-phase flow for the past thirty years, and made an effort to clarify the behavior. Non-Darcy flow behavior, phenomena occurred in primary recovery method of reservoirs that have an API degree gravity of less than 20. It was confirmed that it results in greater production. The compressibility of foam fits to be the one of the general fundamental factor that directs the lifetime of a non-Darcy form of two phase flow behavior or also is known as the foamy oil. In the process of usual drive depletion, foamy oil featured of low production GOR and high daily production rate. Foamy oil is more compressible than conventional solution gas due to the oil that gas dispersed in it; as a result, oil formation volume factor is much higher than that in conventional oil. This paper represents a laboratory data followed by some of the analysis related to the properties of non-Darcy form of two phase flow and that is the compressibility parameter. The experimental results showed that at different saturation pressures and at a room temperature, the trends fit the expected behavior above the saturation pressures. Moreover, the measurements of live oil compressibility were also attempted below the saturation pressures. It was concluded that other properties such as the viscosity is added a significant effect rather than compressibility in the behavior of what so called foamy oil compared to the presence or absence of asphaltenes and other polar oil components.

Keywords: Capillary number; Depletion test; Foamy oil property; Solution gas drive.

1. Introduction

Over almost the last three decades Foamy oil behavior has been studied by different researchers and scholars. Indeed, foamy oil expression typically is indirect to what is known as heavy oil at the reservoir conditions somewhere it was found that crude oil is more viscous than refined mineral oil [1]. Further experimental studies conducted by Busahmin and Maini e.g. related to foam stability and came up with that the non-Darcy of two phase flow performance is adversely impacted by non-produced gas-oil-ratio, however high compressibility makes the system highly nonlinear and created a time dependent model to predict volumes entrained and found the compressibility of foamy oil [2]. Much of the engineering aspects that is involved in the development and exploration of reservoirs worldwide depends on physical properties of fluid especially compressibility and density of heavy oil. The process parameter influence the solution gas performance, and hence they need to optimize using hybrid evolutionary techniques [3-6].

The recent studies analysed oil recovery behavior of crude oil and the mineral oil under solution gas drive under different depletion rates and compressibility [7]. These studies reported about the compressibility of the gas-dispersed oil in it is greater than the oil containing dissolved gas. Few studies carried out research studies to estimate compressibility of foamy oil used simple model correlations [8]. It was suggested by Busahmin and Maini [9] where the drive energy to oil flow dramatically reduces the fractional flow of gas. Foamy oil viscosity, compressibility and permeability were presented by Zhang et al. [10]. In the phase of production, the average capillary number shows large fluctuations. These fluctuations result from changes between the constant recovery of gas and the recovery of non-Darcy two-phase flow behaviour [11]. Production of non-thermal technique has developed over many years; Figure 2 represents an example of heavy oil that features high viscous reservoir with a net pay. It is a feasible technique for oil, water, gas and sand production along with in a primary (non-thermal) recovery process, a practical reservoir example of that is in Lloydminster- Canada [12].

2. Experimental setup

A. Determination of Dead Oil Compressibility

Dead oil compressibility for both refined crude and mineral oil were measured using the densitometer (Paar DMA 45) and the schematic of the measurement is shown in Figure 1. Initially the dead oil was pumped into the densitometer by using the transfer vessel equipped with mini pump and then the oil was compressed at different absolute pressures and the densities were monitored at different pressures.

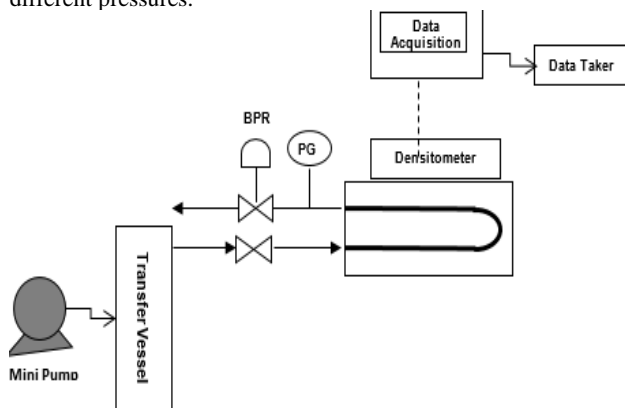


Fig. 1. The Compressibility Set-up at Room Temperature

B. Determination of Live oil compressibility

The compressibility of the live oil was measured using the same experimental set-up following the same procedure followed to determine the compressibility of dead oil. The compressibility of live oil was determined at different saturation pressures and constant room temperature, 25°C.

After placing the live oil in the densitometer and recording a steady state value above the desired saturation pressure, immediately the globe valve between the densitometer and the oil supply transfer vessel was closed off. Then, the valve to the back-pressure regulator (BPR) was opened with its system pressure set at the saturation pressure and the corresponding density is recorded. Then, by reducing the system pressure to a lower pressure which is below the saturation pressure of oil, the corresponding density was also measured. Subsequently the pressure was steadily further reduced and the density variations at each pressure were recorded. This procedure is repeated until the density readings became unstable due to gas evolution.

Table 1: Experimental fluid data for mineral and crude oils

Parameter	Mineral oil	Crude oil	Saturated mineral oil	Saturated crude oil
saturation pressure[psi]	8	N/A	500	500
viscosity @ 23°C [m.Pa.s]	1583	2608	1080	1300
liquid Phase compressibility [psi ⁻¹ , 10 ⁶]	6.80	6.90	4.52	4.37
solution gas oil ratio [cm ³ /cm ³]	N/A	N/A	9.1	10

Table 2: Compressibility data for methane saturated mineral oil

Pressure, psi	Density, kg/m ³	Pressure difference, Δp	Density, g/cm ³	Compressibility, 10 ⁶ psi ⁻¹
500	890.6527	20	0.0785	4.40688
520	890.7312	20	0.0416	2.33516
540	890.7728	20	0.1015	5.69730
560	890.8743	20	0.0832	4.66957
580	890.9575	20	0.0785	4.40537
600	891.0360	20	0.0831	4.66311
620	891.1191	20	0.0877	4.92078
640	891.2068	20	0.0831	4.66222
660	891.2899	20	0.0785	4.40373
680	891.3684	20	0.0878	4.92501
700	891.4562	20	0.0877	4.91892
720	891.5439	20	0.0739	4.14450
740	891.6178	20	0.0831	4.66007
760	891.7009	20	0.0831	4.65963
780	891.7840	20	0.0669	3.74474
800	891.8507	20	0.0810	4.54168
820	891.9318	20	0.0877	4.91630
840	892.0195	20	0.0877	4.91581
860	892.1072	20	0.0785	4.39970
880	892.1857	20	0.0785	4.39931
900	892.2642	20	0.0785	4.39892

Table 3: Compressibility Data for methane saturated crude oil as a function of density and pressure

Pressure, psi	Density, kg/m ³	Pressure difference, Δp	Density, g/cm ³	Compressibility, 10 ⁶ psi ⁻¹
500	927.9647	20	0.0461	2.48393
520	928.0108	20	0.0830	4.47193
540	928.0938	20	0.0645	3.47486
560	928.1583	20	0.1244	6.70144
580	928.2827	20	0.0875	4.71300
600	928.3702	20	0.0737	3.96932
620	928.4439	20	0.0737	3.96901
640	928.5176	20	0.1014	5.46032
660	928.6190	20	0.0783	4.21594

680	928.6973	20	0.1014	5.45926
700	928.7987	20	0.0967	5.20565
720	928.8954	20	0.0553	2.97665
740	928.9507	20	0.0830	4.46741
760	929.0337	20	0.0691	3.71892
780	929.1028	20	0.0829	4.46129
800	929.1857	20	0.0829	4.46090
820	929.2686	20	0.0783	4.21299
840	929.3469	20	0.0784	4.21802
860	929.4253	20	0.0783	4.21228
880	929.5036	20	0.0829	4.45937
900	929.5865	20	0.0829	4.45919

Table 3: Compressibility Data for ethane saturated mineral oil below the saturation pressure, 270 psi

Pressure, psi	Density, kg/m ³	Pressure difference, Δp	Density, g/cm ³	Compressibility, 10 ⁶ psi ⁻¹
60	860.6418	20	0.8606	2.48393
80	860.7436	20	0.8607	4.47193
100	860.8361	20	0.8608	3.47486
120	860.9286	20	0.8609	6.70144
140	861.0211	20	0.8610	4.71300
160	861.0813	20	0.8611	3.96932
180	861.1368	20	0.8611	3.96901
200	861.2062	20	0.8612	5.46032
220	861.2617	20	0.8613	4.21594
240	861.3126	20	0.8613	5.45926
250	861.3033	20	0.8613	5.20565
260	861.2848	20	0.8613	2.97665
270	861.8168	20	0.8618	4.46741

3. Salient features of a heavy oil

This section reviews the most significant physical properties of foamy oil flow including: compressibility, viscosity, surface tension, capillary number foam and foam stability.

A. Compressibility

Compressibility it's a non-equilibrium fluid property and the compressibility of the oil and gas dispersion is greater than solution gas [13]. Few studies carried out research studies to estimate compressibility of foamy oil. As per Kumar and Mahadevan [14], with known foamy oil properties, Foamy oil compressibility can affect pressure responses considerably.

B. Viscosity

Parallel solution gas drive experiments were conducted with a heavy crude oil from reservoir and a de-asphalted version of the

E. Foamy oil Mechanism

The whole process leading to the formation of a gas-in-oil dispersion: Supersaturation, critical supersaturation, Bubble nucleation, Bubble growth, and Bubble movement, or bubble migration

$$S = P_e - P \quad (1)$$

Where: S- Supersaturation, P_e-Equilibrium Pressure, and P- System Pressure

$$J(t) = A \cdot \exp\left(\frac{-B}{\Delta P_s}\right) \quad (2)$$

Where: J(t) Nucleation Rate, A & B Constants, and ΔP_s – Super Pressure difference.

same oil and to eliminate the influence of oil viscosity, the original crude oil was diluted with a 50-50 mixture of heptane and toluene to reduce the viscosity to the same level as that of the de-asphalted oil. The experiments were carried out in a visual sand pack that permitted observation of the bubble formation in the sand. The results show that the effect of asphaltene content varies with the depletion rate. At higher depletion rates, the oil recovery and production profile of crude oil with asphaltene is different from those without asphaltenes [15].

The values of apparent viscosity inferred from applications of classical solution-gas drive models to match the production performance are broadly less than that of those with gas behavior [16]. No exploratory check of this component has been accounted for so far in open writing. However, colloidal properties of asphaltenes and pitches have been the subject of extreme verbal confrontation in the writing. Moreover the substance of asphaltene is one of the principle criteria for the procedure control and the technique to move these oils will relies upon oil properties that incorporate thickness, API gravity, asphaltene content, what's more its capability to yield high esteem items after the refining procedure [17, 18]. The noticeable components that are contemplated by Abusahmin et al. [19] involved refined mineral oil versus raw petroleum frameworks, the parameters incorporate; immersion weight, weight exhaustion rate, and weight drawdown. Both mineral and unrefined petroleum frameworks showed comparable decrease in the oil recuperation execution with diminishing rate of weight consumption [20].

C. Capillary Number

Many researchers have proposed different definitions for capillary number that all represent the ratio. The value of the capillary forces is a function of interfacial tension between the two phases as well as the pore geometry and the wettability conditions.

Often, the capillary number is expressed as:

$$N_{ca} = \frac{k}{\sigma} \frac{dP}{dx}$$

Where σ- the interfacial tension between the wetting and non-wetting fluid, "k" is the absolute permeability and (dP/dx) is the pressure gradient.

D. Determination of fluid properties

Two types of oil systems named crude oil saturated gas and artificial oil saturated gas were used along in the determination of fluid properties at various saturation pressures, these properties include compressibility as shown in Table 1.

$$G(t) = (\omega + \nu) \cdot K \cdot [s^w(t)] t^{(\omega + \nu - 1)} \quad (3)$$

Where: G-Growth Rate, K-Kinetic Constant, and ω, ν – Positive Constants and t-Time

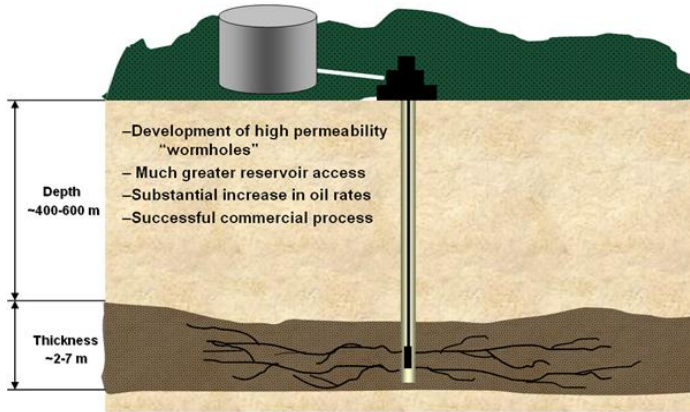


Fig. 2. Cold production Schematic.

4. Results and discussions

These experimentally found data were plotted on a P-ρ graph, where the slope of the least square fitted line was used to calculate the compressibility. The plots for P-ρ for mineral and the crude oil compressibility data are depicted in Figure's 3 and 4 respectively. Crude oil from Grimbek field in Argentina was found slightly compressible than the Catenex, mineral oil used and that is may contain some asphaltene content.

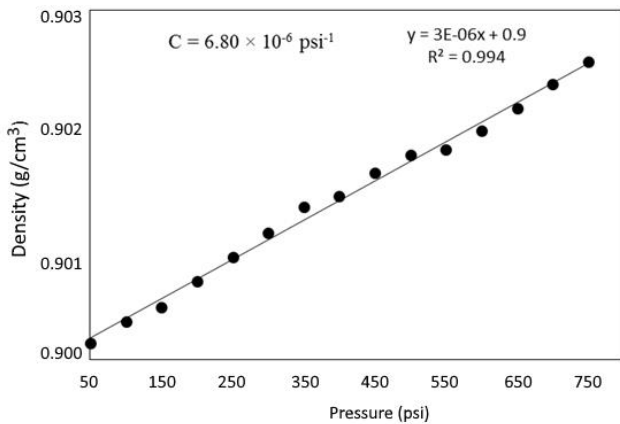


Fig. 3. Refined mineral oil compressibility curve at room temperature, 25-degree C

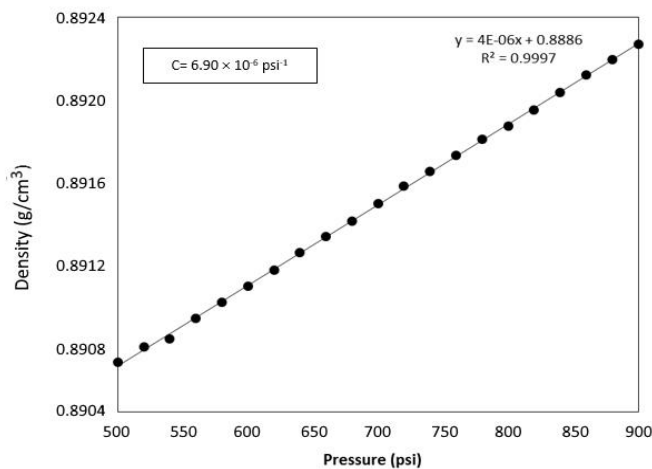


Fig. 4. Crude oil compressibility curve at room temperature at 25-degree C

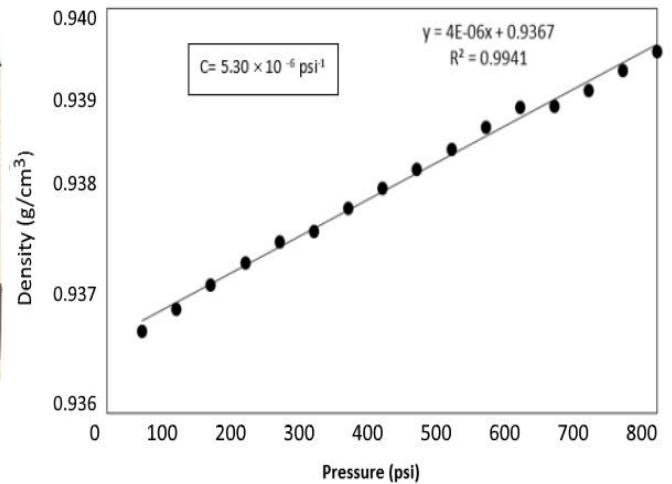


Fig. 5. Methane gas saturated mineral oil compressibility data at room temperature

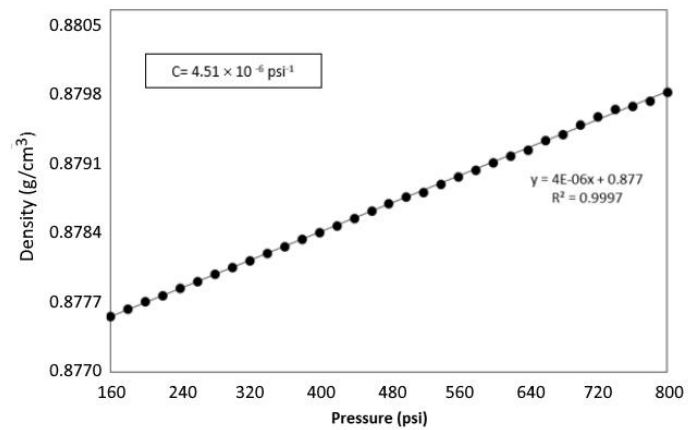


Figure 6 Carbon dioxide gas saturated mineral oil compressibility data at room temperature

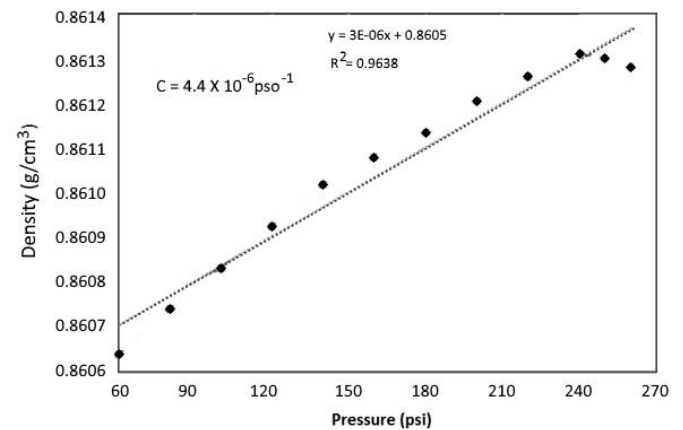


Fig. 7. Ethane saturated mineral oil compressibility data below the saturation pressure, 270 psi at room temperature

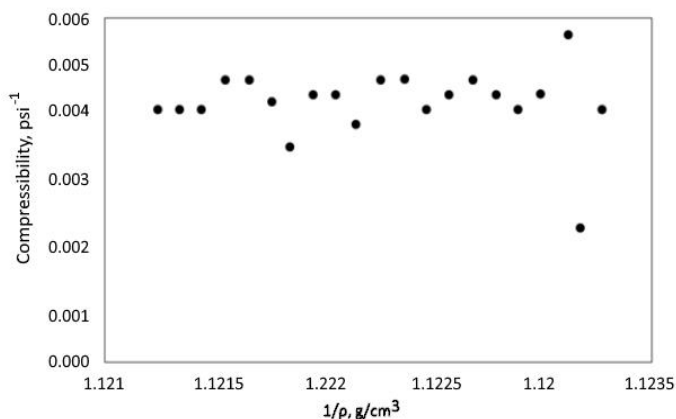


Fig. 8. Compressibility vs density using methane saturated mineral oil

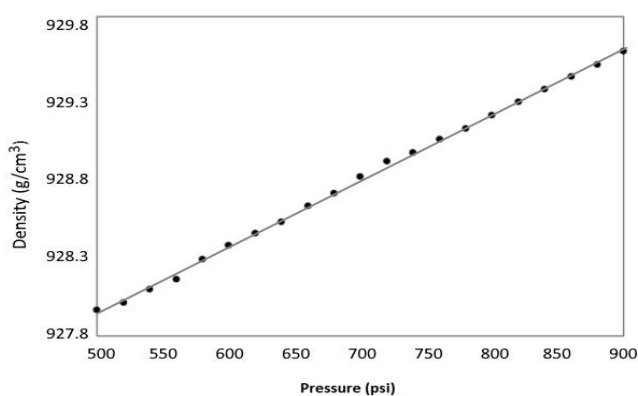


Fig. 9. Pressure and density profiles using methane-saturated crude oil

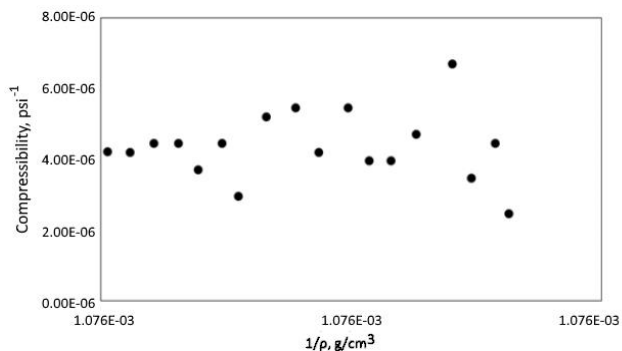


Fig. 10. Compressibility vs density using methane saturated crude oil

Figure's 5 and 6 represents the pressure, density history for methane saturated mineral gas system, carbon dioxide saturated mineral system and the trends, and variation follows the expected behaviour at the saturation pressures. Foamy oil compressibility maybe influenced by pressure reaction considerably related to density and prevailing pressure conditions. The trend of pressure versus density below the saturation pressure is depicted in Figure 7. The compressibility using ethane system is the highest among other gases, due to the gas nucleation and the nature of ethane gas, which can lead to a variation in saturation pressure, made a difference in performance. Figures 8 and 9 presents Compressibility as a function of density utilizing CH₄ saturated mineral and crude oil at the same conditions. Figure 10 depicts the pressure history and density profiles using methane-saturated crude oil.

5. Conclusions

In this study, the pressure for methane and carbon dioxide was kept at the same pressure conditions whereas for ethane it was kept at 270 psi. The compressibility data for ethane-oil system looks much better than for methane oil system, and that is because of gas behavior in the oil system. The trend fits the expected behaviour at the saturation pressure. Non-Darcy form of two-phase flow behavior possibly will be more compressible. The flow of Non-Darcy form of two-phase behavior appears different from the traditional reservoirs. Asphaltene content did not have much impact to Non-Darcy form of two-phase behavior compressibility. Both systems demonstrated comparable results in the compressibility performance at the same saturation pressure as a function of density and pressure.

References

- [1] B.S. Busahmin & B.B. Maini (2011), Comparison between Foamy mineral oil and crude Oil under Solution - gas drive, in: Oil and gas conference, Calgary, Alberta, Canada.
- [2] L. Xiao & G. Zhao (2013), Integrated Study of Foamy Oil Flow and Wormhole Structure in CHOPS through Transient Pressure Analysis, in: SPE Heavy Oil Conference-Canada, Society of Petroleum Engineers.
- [3] K.R. Rao, D.P. Rao, C. Venkateswarlu (2009), Soft sensor based nonlinear control of a chaotic reactor, IFAC Proceedings Volumes, 42, 537-543.
- [4] R.R. Karri, J.N. Sahu (2018), Modeling and optimization by particle swarm embedded neural network for adsorption of zinc (II) by palm kernel shell based activated carbon from aqueous environment, Journal of Environmental Management, 206, 178-191.
- [5] R.R. Karri, J.N. Sahu, N.S. Jayakumar (2017), Optimal isotherm parameters for phenol adsorption from aqueous solutions onto coconut shell based activated carbon: Error analysis of linear and non-linear methods, Journal of the Taiwan Institute of Chemical Engineers, 80, 472-487.
- [6] K.R. Rao, T. Srinivasan, C. Venkateswarlu (2010), Mathematical and kinetic modeling of biofilm reactor based on ant colony optimization, Process Biochemistry, 45,961-972.
- [7] B. Busahmin, B. Maini, R.R. Karri, M. Sabet (2017), Studies on the Stability of the Foamy Oil in Developing Heavy Oil Reservoirs, Defect and Diffusion Forum, 371,111-116.
- [8] J.G. Sheng, B.B. Maini, W.S. Tortike (1995), A Non-Equilibrium Model to Calculate Foamy Oil Properties, in: Annual Technical Meeting, Petroleum Society of Canada.
- [9] B.B. Maini & B. Busahmin (2010), Foamy oil flow and its role in heavy oil production, in: AIP Conference Proceedings, AIP, 103-108.
- [10] X. Zhang, X. Wu, J. Zhang, R. Wang, L. Wang, R. Zhao, K. Liu (2012), A New Modeling Approach for Bubble Growth in Foamy Oil, Petroleum Science and Technology, 30, 1498-1507.
- [11] B. Busahmin, B. Maini, U.H.B.H. Hasan (2017), Influence of Compressibility on Heavy/FoamyOil Flow, IOSR Journal of Engineering, 07, 18-28.
- [12] M. Tavallali, B.B. Maini, T.G. Harding, B.S. Busahmin 2012, Assessment of SAGD Well Configuration Optimization in Lloydminster Heavy Oil Reserve, in: SPE/EAGE European Unconventional Resources Conference and Exhibition, Society of Petroleum Engineers.
- [13] Hemmati-Sarapardeh, A. and Mohagheghian, E., Modeling interfacial tension and minimum miscibility pressure in paraffin-nitrogen systems: Application to gas injection processes. Fuel, Vol. 205 No., (2017), 80-89.
- [14] Y. Shi, X. Li, D. Yang (2016), Nonequilibrium Phase Behavior of Alkane Solvent(s) -CO₂-Heavy Oil Systems under Reservoir Conditions, Industrial & Engineering Chemistry Research, 55, 2860-2871.
- [15] R. Kumar, J. Mahadevan (2012), Well-performance relationships in heavy-foamy-oil reservoirs, SPE Production & Operations, 27, 94-105.

- [16] X. Sun, Y. Zhang, S. Wang, Z. Song, P. Li, C. Wang (2018), Experimental study and new three-dimensional kinetic modeling of foamy solution-gas drive processes, *Scientific reports*, 8, 4369.
- [17] G.E. Smith, *Fluid Flow and Sand Production in Heavy-Oil Reservoirs Under Solution-Gas Drive*, *SPE Production Engineering*, 3 (1988) 169-180.
- [18] E.L. Claridge (1994), A proposed model and mechanism for anomalous foamy heavy oil behavior.
- [19] R.G. Santos, W. Loh, A.C. Bannwart, O.V. Trevisan (2014), An overview of heavy oil properties and its recovery and transportation methods, *Brazilian Journal of Chemical Engineering*, 31, 571-590.
- [20] B.S. Abusahmin, R.R. Karri, B.B. Maini (2017), Influence of fluid and operating parameters on the recovery factors and gas oil ratio in high viscous reservoirs under foamy solution gas drive, *Fuel*, 197, 497-517.
- [21] B. Busahmin, E.-S.M. Zahran, B. Maini (2016), Application of Foamy Mineral Oil Flow under Solution Gas Drive to a Field Crude Oil, *The International Journal of Engineering and Science (IJES)*, 5, 48-58.